

# Acidic cesium salts of 12-tungstophosphoric acid as catalysts for the dehydration of xylose into furfural

Ana S. Dias, Sérgio Lima, Martyn Pillinger and Anabela A. Valente\*

*Department of Chemistry, CICECO, University of Aveiro, Campus de Santiago, 3810-193 Aveiro, Portugal*

Received 27 July 2006; accepted 10 October 2006

Available online 17 October 2006

**Abstract**—Cesium salts of 12-tungstophosphoric acid,  $\text{Cs}_x\text{H}_{3-x}\text{PW}_{12}\text{O}_{40}$  ( $\text{Cs}_x\text{PW}$ ), in the bulk form or supported on medium-pore MCM-41 (3.7 nm) or large-pore (9.6 nm) micelle-templated silicas are active solid acid catalysts for the cyclodehydration of xylose into furfural, in a toluene/water solvent system (T/W) or in dimethyl sulfoxide (DMSO). The catalytic results are comparable to those obtained using sulfuric acid, under similar reaction conditions. The initial activities increase in the order  $\text{H}_3\text{PW}_{12}\text{O}_{40} < \text{Cs}_{2.0}\text{PW} < \text{Cs}_{2.5}\text{PW} < \text{silica-supported CsPW catalysts (15, 34 wt \% PW)}$ . Higher HPA loadings, larger pore diameter of the parent silica support, and higher reaction temperatures lead to higher furfural yields. The stability and reusability of the MCM-41-supported CsPW is higher in DMSO than in T/W.

© 2006 Elsevier Ltd. All rights reserved.

**Keywords:** Xylose; Furfural; Dehydration; Solid acid catalysis; Cesium salts; Heteropolyacid; 12-Tungstophosphoric; Mesoporous silicas; MCM-41

## 1. Introduction

Biomass is one of the world's most important renewable energy sources. As carbohydrates represent 75% of the annually renewable biomass of about 200 billion tons, their utilization for the generation of organic chemicals that eventually replace those derived from petrochemical resources is a major challenge for green chemistry.<sup>1,2</sup> With an annual production of approximately 250,000 tons, 2-furaldehyde (furfural) seems to be the only unsaturated large-volume organic chemical prepared from carbohydrate sources.<sup>3,4</sup> Furfural is a highly versatile and key derivative used in the manufacture of a wide range of important chemicals, and is likely to be of increasing demand in different fields, such as oil refining, plastics, pharmaceutical and agrochemical industries. The technical process for the production of furfural involves the acid catalyzed hydrolysis of the hemicellulosic pentose fractions of biomass (such as cornstalks and

corncoobs, oat and peanut husks, and other agricultural surpluses) and consecutive cyclodehydration of the pentose monomers (xylose being the most predominant pentose in most feedstocks).<sup>3</sup> Conventional mineral acids, such as sulfuric acid, are generally used as the catalysts. The cost and inefficiency of separating these catalysts from the products makes their recovery impractical, resulting in large volumes of acid waste, which must be neutralized and disposed off. Other drawbacks include corrosion and safety problems. The production of furfural is therefore one of many industrial processes where the replacement of the 'toxic liquid' acid catalysts by alternative 'green' catalysts is of high priority.<sup>5,6</sup>

Heteropolyacids (HPAs) are promising candidates as green catalysts and are already used in several industrial processes, such as the hydration of olefins.<sup>7–12</sup> We recently reported that 12-tungstophosphoric acid ( $\text{H}_3\text{PW}_{12}\text{O}_{40}$ , abbreviated as HPW) is comparable to  $\text{H}_2\text{SO}_4$  for the cyclodehydration of xylose into furfural, in a homogeneous phase.<sup>13</sup> It would be preferable, however, if the reaction could be carried out in a heterogeneous phase, in order to facilitate product separation, catalyst recovery and recycling. Unfortunately, in the

\* Corresponding author. Tel.: +351 234 378123; fax: +351 234 370084; e-mail: [avalente@dq.ua.pt](mailto:avalente@dq.ua.pt)

solid-state HPW is a nonporous material with a surface area below  $10 \text{ m}^2 \text{ g}^{-1}$ , and is soluble in polar solvents. In order to overcome this limitation one can prepare acid salts containing large cations such as  $\text{Cs}^+$ ,  $\text{K}^+$ ,  $\text{Rb}^+$ , and  $\text{NH}_4^+$ , which present surface areas as high as  $150 \text{ m}^2 \text{ g}^{-1}$ .<sup>12,14–17</sup> Of these, the water-tolerant, insoluble, acidic Cs salt,  $\text{Cs}_{2.5}\text{H}_{0.5}\text{PW}_{12}\text{O}_{40}$  (abbreviated as  $\text{Cs}_{2.5}\text{PW}$ ), has the highest specific surface acidity, and is an efficient solid acid catalyst for a variety of organic reactions, such as the liquid-phase dehydration of alcohols and hydrolysis of esters.<sup>8,11,18–21</sup> A problem associated with the use of  $\text{Cs}_x\text{PW}$  catalysts is that the salt particles disperse as a colloid in water and in many organic solvents, making it difficult to separate the salt from the reaction products by simple filtration.<sup>11</sup> The dispersion of Cs salts on a carrier with a high specific surface area may eliminate the difficulty of the separation and work-up procedures, and can enhance the activity of salts with low Cs content (such as  $\text{Cs}_{2.0}\text{PW}$ , which possesses lower specific surface acidity as a result of a reduced specific surface area) by exposing more of the acid sites to the catalytic reaction.<sup>22</sup>

In the present work, bulk and mesoporous silica-supported  $\text{Cs}_x\text{PW}$  salts were studied as catalysts for the cyclodehydration of xylose into furfural. We chose the micelle-templated silica MCM-41 as a support because there is evidence that  $\text{CsPW}$  salts interact more strongly with MCM-41 than with  $\text{SiO}_2$ ,<sup>22</sup> and it has been demonstrated that the generation of insoluble acidic cesium salts inside the channels of MCM-41 prevents leaching of the active phase.<sup>22–24</sup> In order to assess the possible blocking of the regular pores of MCM-41 by the Keggin ions, we have also used a mesoporous silica with a pore size of 9.6 nm as the support.

## 2. Experimental

### 2.1. Catalyst preparation

**2.1.1.  $\text{Cs}_x\text{H}_{3-x}\text{PW}_{12}\text{O}_{40}$  ( $\text{Cs}_x\text{PW}$ ).** A 0.1 M aqueous solution of  $\text{Cs}_2\text{CO}_3$  ( $20 \text{ cm}^3$  for  $x = 2.5$  and  $12.7 \text{ cm}^3$  for  $x = 2.0$ ) was added dropwise to a 0.08 M aqueous solution of 12-tungstophosphoric acid hydrate ( $20 \text{ cm}^3$  for  $x = 2.5$  and  $15.9 \text{ cm}^3$  for  $x = 2.0$ ) at room temperature, under vigorous stirring.<sup>15</sup> The resultant milky suspensions were aged at room temperature overnight. White powders were isolated by slow evaporation of water at  $50^\circ\text{C}$ .

**2.1.2. Impregnation of acidic cesium salts of  $\text{H}_3\text{PW}_{12}\text{O}_{40}$  in the porous silica supports.** Full details concerning the syntheses of the mesoporous silica supports are given in Refs. 25–27. The medium-pore (MP) micelle-templated silica (MTS) was synthesized from a gel with the molar composition  $\text{SiO}_2:0.29\text{Na}_2\text{O}:0.50\text{C}_{16}\text{TMABr}:150\text{H}_2\text{O}$ ,

where  $\text{C}_{16}\text{TMABr}$  is cetyltrimethylammonium bromide.<sup>25,26</sup> Calcination of the as-synthesized material was carried out at  $560^\circ\text{C}$  for 6 h under a static atmosphere of air. Powder XRD ( $2\theta/^\circ$ ,  $hkl$  in parentheses): 2.46 (100), 4.21 (110), 4.81 (200), 6.28 (210);  $a = 2d_{100}/\sqrt{3} = 41.4 \text{ \AA}$ . The large-pore (LP) MTS was synthesized from a gel with the molar composition  $\text{SiO}_2:0.271\text{Na}_2\text{O}:0.116\text{C}_{16}\text{TMACl}:0.025\text{C}_{12}\text{TMABr}:0.75\text{-mesitylene}:30.3\text{H}_2\text{O}$ , where  $\text{C}_{12}\text{TMABr}$  is dodecyltrimethylammonium bromide.<sup>26,27</sup> Calcination was carried out at  $120^\circ\text{C}$  for 3 h and then at  $560^\circ\text{C}$  for 4 h.

Highly dispersed Cs-tungstophosphoric acid salts on mesoporous silicas, denoted as  $\text{MP}_x\text{CsPW}$  ( $x = 15$  or  $34 \text{ wt \% PW}$ ) and  $\text{LP15CsPW}$ , were prepared following the two-step impregnation technique described by Wang et al.<sup>28</sup> First, the purely siliceous MP or LP supports (1 g) were added to a solution of  $\text{Cs}_2\text{CO}_3$  (10 or 35 mg, 0.03 or 0.11 mmol) in water ( $10 \text{ cm}^3$ ) and the mixtures were stirred overnight at room temperature. The mixtures were then evaporated to dryness at  $110^\circ\text{C}$  overnight and the resultant solids calcined at  $500^\circ\text{C}$  for 2 h, to promote interactions between surface silanols and  $\text{Cs}_2\text{CO}_3$ . Following this, the desired amount of HPW (to give a final Cs:P molar ratio of 1:1) was impregnated by the incipient wetness technique, using 1-butanol as a solvent.

### 2.2. Catalyst characterization

ICP-AES was carried out at the Central Laboratory for Analysis, University of Aveiro (by E. Soares). Powder XRD data were collected at room temperature on a Philips X'pert diffractometer with a curved graphite monochromator ( $\text{Cu K}_\alpha$  radiation), in a Bragg-Brentano para-focusing optics configuration. Samples were step-scanned in  $0.05^\circ 2\theta$  steps with a counting time of 1 s per step. Differential scanning calorimetry (DSC) was performed under air with a Shimadzu DSC-50 system at a heating rate of  $5^\circ\text{C min}^{-1}$ . BET specific surface areas ( $S_{\text{BET}}$ ,  $p/p_0$  from 0.03 to 0.13) and specific total pore volumes,  $V_t$ , were estimated from  $\text{N}_2$  adsorption isotherms measured at  $-196^\circ\text{C}$ . For the large-pore support an automatic ASAP 2000 adsorption apparatus was used, and for the medium-pore support a gravimetric adsorption apparatus equipped with a CI electronic MK2-M5 microbalance and an Edwards Barocel pressure sensor was used.  $^{29}\text{Si}$  and  $^{31}\text{P}$  solid-state MAS NMR spectra were recorded at 79.49 and 161.90 MHz, respectively, on a 9.4 T Bruker Avance 400 spectrometer.  $^{29}\text{Si}$  MAS NMR spectra were recorded with  $40^\circ$  pulses, a spinning rate of 5.0 kHz, and 60 s recycle delays.  $^{29}\text{Si}$  CP MAS NMR spectra were recorded with  $5.5 \mu\text{s } ^1\text{H } 90^\circ$  pulses, a contact time of 8 ms, a spinning rate of 5.0 kHz, and 4 s recycle delays.  $^{31}\text{P}$  MAS NMR spectra were recorded with  $40^\circ$  pulses, a spinning rate of 15.0 kHz, and 70 s recycle delays. Chemical shifts

are quoted in parts per million from TMS for the  $^{29}\text{Si}$  spectra and from phosphoric acid (85%  $\text{H}_3\text{PO}_4$ ) for the  $^{31}\text{P}$  spectra.

### 2.3. Catalytic reactions

The catalytic experiments were performed under nitrogen in a magnetically stirred batch micro-reactor equipped with a valve for gas purging (mixing speeds  $\geq 500$  rpm), and heated with a thermostatically controlled oil bath. In a typical procedure, D-xylose (30 mg, 0.20 mmol), powdered catalyst (30 mg), and DMSO (1  $\text{cm}^3$ ) or, in the case of a solvent mixture, water (0.3  $\text{cm}^3$ ) and toluene (0.7  $\text{cm}^3$ ) were poured into the reactor. Zero time was taken to be the instant the micro-reactor was immersed in the oil bath. Throughout this work, selectivity always refers to the formation of furfural and conversion refers to xylose consumption.

The products in the DMSO or aqueous phases were analyzed using a Knauer K-1001 HPLC pump and a PL Hi-Plex H 300  $\times$  7.7 (i.d.) mm ion exchange column (Polymer Laboratories Ltd., UK), coupled to a Knauer K-2401 differential refractive index detector (for xylose) and a Knauer K-2600 UV detector (280 nm, for furfural). The mobile phase was 0.01 M  $\text{H}_2\text{SO}_4$ . A flow rate of 0.6  $\text{cm}^3 \text{min}^{-1}$  and a column temperature of 65  $^\circ\text{C}$  were used. Authentic samples of D-xylose and furfural were used as standards and calibration curves were used for quantification. When toluene was used as a co-solvent, the furfural present in the organic phase was quantified using a Gilson 306 HPLC pump and a Spherisorb ODS S10 C18 column, coupled to a Gilson 118 UV/Vis detector (280 nm). The mobile phase consisted of 40% v/v MeOH in water (flow rate 0.7  $\text{cm}^3 \text{min}^{-1}$ ).

## 3. Results and discussion

### 3.1. Characterization of the catalysts

Figure 1 shows the powder XRD patterns of the bulk and mesoporous silica-supported Cs-tungstophosphoric acid salts in the  $2\theta$  range of 10–30 $^\circ$ . The patterns for the Cs salts  $\text{Cs}_2\text{HPW}_{12}\text{O}_{40}$  and  $\text{Cs}_{2.5}\text{H}_{0.5}\text{PW}_{12}\text{O}_{40}$  exhibit the characteristic lines of the cubic HPW structure and are in agreement with published data.<sup>15,29,30</sup> Compared with 12-tungstophosphoric acid hydrate (Fig. 1a), the peaks are broader and shifted toward higher angles, consistent with the smaller cubic lattice constants obtained for these compounds in the literature.<sup>15</sup> The XRD patterns for the mesoporous silica-supported materials clearly show the presence of the Cs-acid salt. Paralleling the behavior exhibited by the bulk Cs-acid salt, the reflections for MP15CsPW and LP15CsPW shift slightly to higher  $2\theta$  values relative to  $\text{H}_3\text{PW}_{12}\text{O}_{40} \cdot x\text{H}_2\text{O}$ , indicating contraction of the unit cell as  $\text{H}_5\text{O}_2^+$

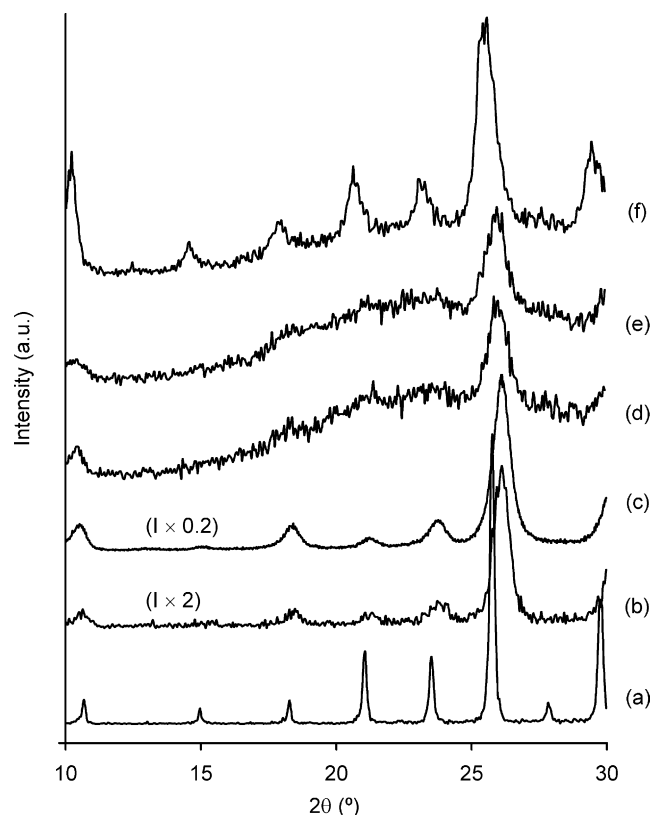


**Figure 1.** Powder XRD patterns of (a) bulk  $\text{H}_3\text{PW}_{12}\text{O}_{40} \cdot x\text{H}_2\text{O}$  ( $x \approx 17$ ), (b)  $\text{Cs}_{2.0}\text{PW}$ , (c)  $\text{Cs}_{2.5}\text{PW}$ , (d) MP15CsPW, (e) LP15CsPW, and (f) MP34CsPW.

ions are replaced by the smaller  $\text{Cs}^+$  ions.<sup>31,32</sup> Surprisingly, the reflections for MP34CsPW shift to slightly lower  $2\theta$  values relative to  $\text{H}_3\text{PW}_{12}\text{O}_{40} \cdot x\text{H}_2\text{O}$ . At the present time, we do not have an explanation for this result.

The textural properties of the Cs-containing catalysts were further drawn from the  $\text{N}_2$  adsorption–desorption isotherms. In agreement with the literature data, the BET specific surface area of the  $\text{Cs}_{2.5}\text{PW}$  salt (128  $\text{m}^2 \text{g}^{-1}$ ) was much higher than that for  $\text{Cs}_{2.0}\text{PW}$  (21  $\text{m}^2 \text{g}^{-1}$ ).<sup>33</sup> The relatively high surface area of the acid salts with a higher amount of Cs has been attributed to the formation of primary particles with smaller sizes possessing inter-crystallite pores.<sup>12,15,34</sup> For  $\text{Cs}_{2.0}\text{PW}$ , the lower specific surface area may be due to the predominance of ultra-micropores.<sup>12,35</sup> The pristine MTS supports exhibited type IV  $\text{N}_2$  adsorption–desorption isotherms according to IUPAC classification (pore width between 2 and 50 nm), typical of mesoporous solids (not shown).<sup>26</sup> The steps corresponding to capillary condensation in the primary mesopores appeared in the relative pressure ranges of 0.2–0.4 and 0.7–0.9 for the MP and LP solids, respectively. For the MP silica, the specific surface area was 775  $\text{m}^2 \text{g}^{-1}$ , the total pore volume was 0.6  $\text{cm}^3 \text{g}^{-1}$ , and the maximum of the pore size distribution curve determined by the BJH method

was 3.7 nm. The corresponding values for the LP silica were  $1106 \text{ m}^2 \text{ g}^{-1}$ ,  $2.9 \text{ cm}^3 \text{ g}^{-1}$ , and 9.6 nm. After supporting HPW on the Cs-modified MP silica, the isotherm changed to type I and lower  $\text{N}_2$  uptakes were observed, resulting in a decrease in the measured specific surface area and pore volume, the decrease being larger as the amount of supported acid increases (Table 1). Taking into account the size of the Keggin anion (ca. 1.2 nm), partial clogging of the monodimensional channels of medium-pore MCM-41 by small aggregates of PW may have occurred.<sup>36</sup> Indeed, when HPW was supported on the Cs-modified large-pore support, the relative decrease in surface area and pore volume was, for a PW loading of 15 wt %, lower as compared with the catalyst prepared from the MP silica (Table 1). The LP15CsPW sample exhibited a type IV isotherm and a median pore diameter of 7.3 nm.

The  $^{29}\text{Si}$  MAS NMR spectrum of the unmodified MP silica exhibits two broad overlapping peaks at  $-101.4$  and  $-109.4$  ppm (Fig. 2), assigned to  $\text{Q}^3$  and  $\text{Q}^4$  species of the silica framework, respectively [ $\text{Q}^n = \text{Si}(\text{OSi})_n(\text{OH})_{4-n}$ ]. A small amount of  $\text{Q}^2$  environments is also present (faint peak at  $\delta = -92$  ppm). A similar spectrum was obtained for the unmodified LP silica (not shown). The  $^{29}\text{Si}$  CP MAS NMR spectrum of the MP silica shows a marked increase in the intensities of the  $\text{Q}^2$  and  $\text{Q}^3$  signals over that for the  $\text{Q}^4$  peak, confirming that the  $\text{Q}^2$  and  $\text{Q}^3$  silicons are attached to hydroxyl groups. After supporting HPW on the Cs-modified MP silica (to give final PW loadings of 15 and 34 wt %), no significant changes were observed in the  $^{29}\text{Si}$  MAS NMR spectra, although there is an apparent decrease in the relative intensities of the  $\text{Q}^2$  and  $\text{Q}^3$  peaks (in the spectra measured without  $^1\text{H}$ – $^{29}\text{Si}$  cross-polarization).

Figure 3 shows the  $^{31}\text{P}$  MAS NMR spectra of 12-tungstophosphoric acid hydrate (HPW),  $\text{Cs}_{2.5}\text{PW}$ , MP15CsPW and MP34CsPW. All of the samples were measured after exposure in ambient atmosphere. Hydrated HPW displays one main peak centered at  $-15.5$  ppm, in agreement with the literature data.<sup>37</sup> It is well known that the  $^{31}\text{P}$  chemical shift of HPW is very sensitive to its hydration level. Hence, the shoulders on the peak at  $-15.5$  ppm are probably due to small variations in the degree of hydration, locally experienced by phosphorus. The sample  $\text{Cs}_{2.5}\text{PW}$  shows a single peak

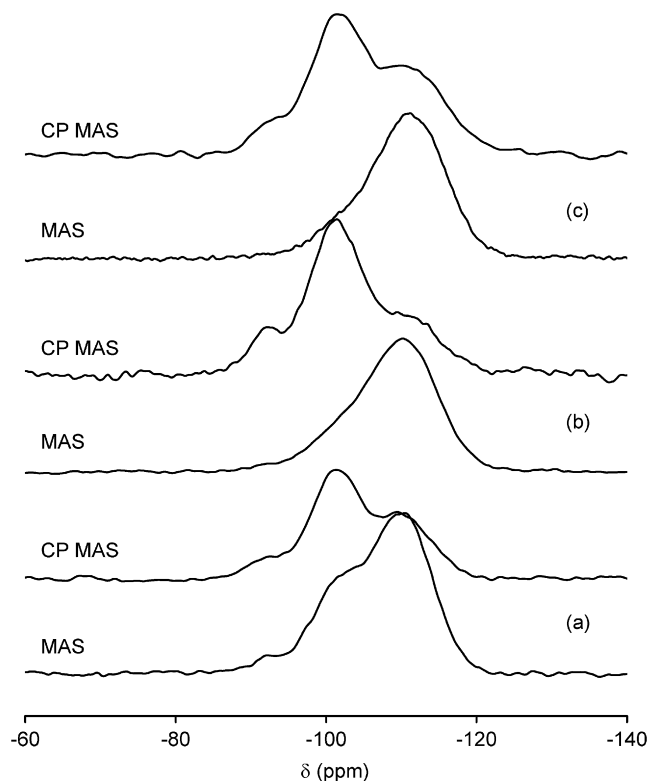


Figure 2.  $^{29}\text{Si}$  MAS and CP MAS NMR spectra of (a) pristine calcined MP-silica (MCM-41), (b) MP15CsPW, and (c) MP34CsPW.

at  $-15.0$  ppm, as for the neutral salt  $\text{Cs}_3\text{PW}_{12}\text{O}_{40}$ .<sup>19,37</sup> After impregnation of HPW onto the Cs-modified MP silica (to give final PW loadings of 15 and 34 wt %), a slightly broader peak was observed at  $-15.15$  ppm. The broadening of the signal may be due to the coexistence of  $\text{CsH}_2\text{PW}$ ,  $\text{Cs}_2\text{HPW}$ , and  $\text{H}_3\text{PW}$  in various amounts.<sup>30</sup> In conclusion, the spectra confirm that the Keggin structure was retained for the bulk and supported Cs acid salts, and do not show the presence of any other phosphorus-containing impurities or degradation products.

### 3.2. Catalysis

In a biphasic solvent system composed of toluene and water (T/W), under batchwise processing, the xylose

Table 1. Conversion of xylose to furfural in the presence of supported Cs salts of HPW<sup>a</sup>

Catalyst	$\Delta S_{\text{BET}}^b$ (%)	$\Delta V_t^b$ (%)	DMSO (140 °C)		T/W (140 °C)		T/W (160 °C)	
			Conv. (%)	Yield (%)	Conv. (%)	Yield (%)	Conv. (%)	Yield (%)
None	—	—	34	1	2	(<1)	12	2
MP15CsPW	81	73	63	11	36	3	69	14
MP34CsPW	91	92	91	45	34	13	68	33
LP15CsPW	55	49	70	24	38	7	65	26

<sup>a</sup> Reaction time = 4 h.

<sup>b</sup> Percentage decrease of surface area ( $S_{\text{BET}}$ ) and total pore volume ( $V_t$ ) in relation to the parent MP ( $775 \text{ m}^2 \text{ g}^{-1}$ ,  $0.6 \text{ cm}^3 \text{ g}^{-1}$ ) and LP ( $1106 \text{ m}^2 \text{ g}^{-1}$ ,  $2.9 \text{ cm}^3 \text{ g}^{-1}$ ) materials.



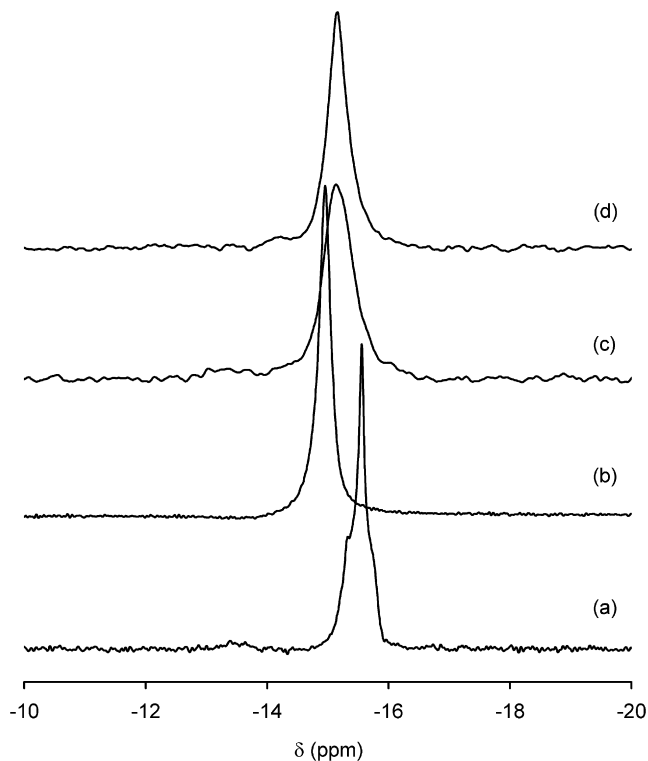
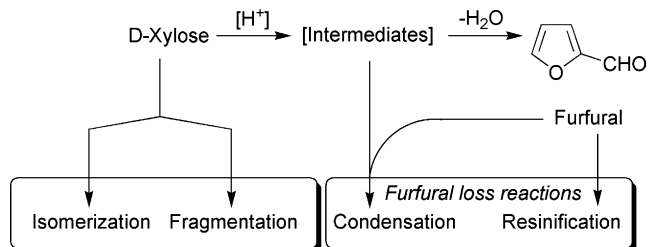


**Figure 3.**  $^{31}\text{P}$  MAS NMR spectra of (a)  $\text{H}_3\text{PW}_{12}\text{O}_{40}\cdot x\text{H}_2\text{O}$  ( $x \approx 17$ ), (b)  $\text{Cs}_{2.5}\text{PW}$ , (c)  $\text{MP15CsPW}$ , and (d)  $\text{MP34CsPW}$ .

conversion proceeds predominantly in the aqueous phase where it is completely dissolved, and furfural, which has a higher affinity for toluene, may be separated from xylose and polar intermediates as it is formed. As a result, the T/W system leads to higher furfural yields than if only water is used as a solvent.<sup>13</sup> Similar results have been recently reported for the fructose-to-hydroxymethylfurfural conversion.<sup>38</sup> The overall reaction may be summarized as shown in Scheme 1. According to the literature, the reaction mechanism involves irreversible development of conjugation via the formation of enediol intermediates, leading to the liberation of three water molecules per molecule of furfural formed.<sup>3,39</sup>

All HPA materials prepared in this work were catalytically active for the cyclodehydration of xylose. Control experiments carried out in T/W at 160 °C showed that only minor amounts of furfural (<2% at 4 h) were yielded in the absence of a HPA catalyst, whereas in the presence of a catalyst at least 14% furfural was



**Scheme 1.**

yielded. The MCM-41-type MP silica support is inert under the applied reaction conditions. We have previously shown that the sodium salt  $\text{Na}_3\text{PW}_{12}\text{O}_{40}$  is inactive in a homogeneous phase, suggesting that HPA protons play a leading role in the promotion of the reaction.<sup>13</sup>

The  $\text{Cs}_x\text{H}_{3-x}\text{PW}_{12}\text{O}_{40}$  ( $x = 2.0, 2.5$ ) compounds form a fine suspension in the aqueous phase. In T/W at 160 °C, the initial activity of  $\text{Cs}_{2.5}\text{PW}$ , based on TOF expressed per proton and calculated at 1 h, is 11.6 mol (equiv  $\text{H}^+$ )<sup>-1</sup> h<sup>-1</sup>, which is significantly higher than that observed for bulk  $\text{H}_3\text{PW}_{12}\text{O}_{40}$  (4.0 mol (equiv  $\text{H}^+$ )<sup>-1</sup> h<sup>-1</sup>), which is completely soluble in the aqueous phase with dissociated protons. The  $\text{Cs}_{2.5}\text{PW}$  compound is known to have high activity for acid-catalyzed reactions even in the presence of large excesses of water, which has been attributed to its hydrophobic nature.<sup>9,12,16,40</sup> The initial activity of  $\text{Cs}_{2.0}\text{PW}$  (3.7 mol (equiv  $\text{H}^+$ )<sup>-1</sup> h<sup>-1</sup>) is lower than that of  $\text{Cs}_{2.5}\text{PW}$ . A recent study revealed the presence of similar proton strengths for both  $\text{Cs}_{2.0}\text{PW}$  and  $\text{Cs}_{2.5}\text{PW}$ , based on calorimetry and adsorption of pyridine.<sup>30</sup> Differences in acid properties between  $\text{Cs}_{2.0}\text{PW}$  and  $\text{Cs}_{2.5}\text{PW}$  may exist with respect to the amount of surface acid sites. For  $\text{Cs}_x\text{H}_{3-x}\text{PW}_{12}\text{O}_{40}$  compounds, the acid site concentration reaches a maximum for  $x = 2.5$ .<sup>12</sup> The  $\text{Cs}_{2.5}\text{PW}$  salt adsorbs polar or basic molecules, such as alcohols (xylose), essentially only on the catalyst surface.<sup>9,31</sup> Hence, assuming surface-type catalysis, the higher initial activity of  $\text{Cs}_{2.5}\text{PW}$  in comparison to  $\text{Cs}_{2.0}\text{PW}$  may be due to the higher specific surface area with higher concentration of readily accessible acid sites. Eventually, for reaction times longer than 4 h, xylose conversion is higher for  $\text{Cs}_{2.0}\text{PW}$  than for  $\text{Cs}_{2.5}\text{PW}$  (Fig. 4a). As shown in Figure 4b, furfural selectivity reaches a maximum of about 48% for  $\text{Cs}_{2.5}\text{PW}$  and 65% for  $\text{Cs}_{2.0}\text{PW}$  at about 50% conversion, and then starts to decrease. The generally lower selectivities observed with  $\text{Cs}_{2.5}\text{PW}$  as the catalyst may be due in part to the hydrophobic surface of this material, which may enhance sorption of furfural and formation of condensation by-products that cause catalyst surface passivation (the reaction mixture becomes brown with time).

The kinetic profiles of the silica-supported CsPW catalysts show higher conversion rates than bulk  $\text{Cs}_x\text{PW}$  (Fig. 4a). The initial activities, calculated after 1 h, were 66.2 and 24.0 mol mol<sup>-1</sup><sub>PW</sub> h<sup>-1</sup> for  $\text{MP15CsPW}$  and  $\text{MP34CsPW}$ , respectively, compared with 3.7–5.8 mol mol<sup>-1</sup><sub>PW</sub> h<sup>-1</sup> for the  $\text{Cs}_x\text{PW}$  compounds. The higher initial activity observed for the supported material with the lower PW loading may be due to a higher dispersion of the active phase on the silica host (leading to active site isolation). It must also be considered that pore blocking effects are less severe for this sample (as evidenced by the surface area and pore volume measurements), resulting in a higher number of effective acid

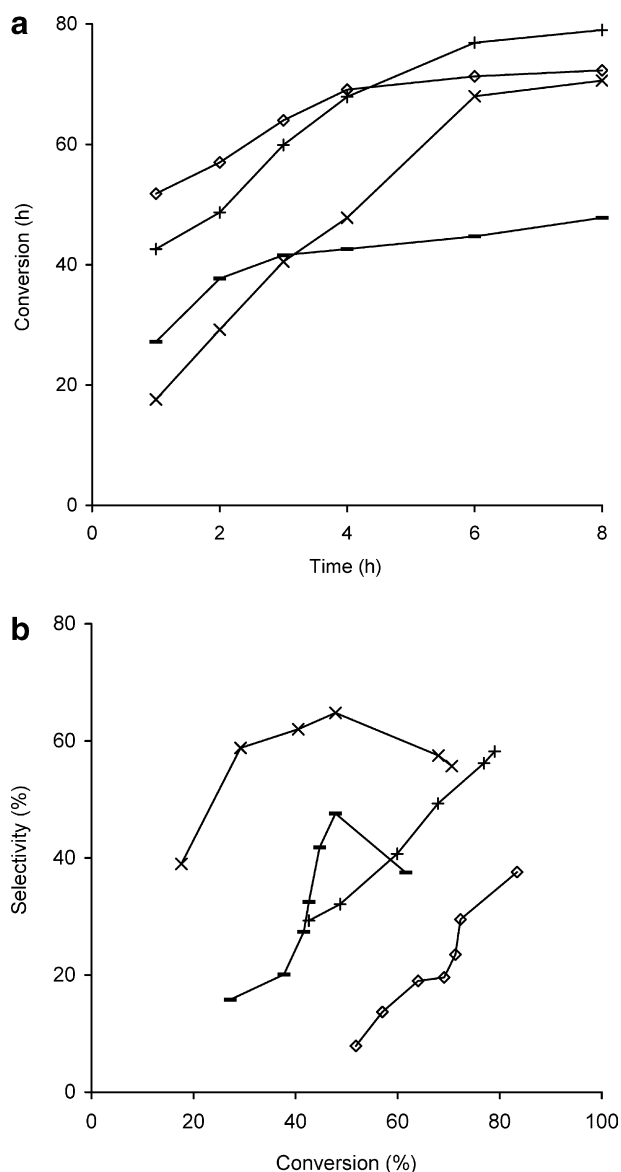


**Figure 4.** Kinetic profiles of xylose conversion (a) and selectivity to furfural as a function of xylose conversion (b) in the presence of Cs<sub>2.0</sub>PW (x), Cs<sub>2.5</sub>PW (—), MP15CsPW (◇), and MP34CsPW (+), in T/W at 160 °C.

sites. The higher activity of CsPW supported on MCM-41 in comparison to bulk Cs<sub>x</sub>PW has been observed for several reaction systems, and is generally attributed to the higher number of effective acid sites present in the supported catalysts.<sup>9,28,31</sup> The HPAs are anchored to the silica support through Cs, which can be achieved with minimum proton substitution, that is, retaining high proton density (for optimized catalytic activity), whereas in the Cs<sub>x</sub>PW bulk forms,  $x = 2.5$  is generally required for optimum surface area, porosity and concentration of proton sites.<sup>9,12</sup>

In contrast to that seen with the Cs<sub>x</sub>PW bulk catalysts, furfural selectivity in the presence of the supported catalysts continues to increase for conversions higher

than 50% (Fig. 4b). This is probably due to the significantly higher residence times (which most likely favor furfural loss reactions) needed for the Cs<sub>x</sub>PW catalysts to achieve the same conversions as the supported catalysts.<sup>3</sup> On the other hand, in the presence of the supported catalysts (but not the bulk Cs<sub>x</sub>PW catalysts), the formation of lyxose was observed, which is an isomerization product of open-chain xylose that may subsequently be converted into furfural (Scheme 1).<sup>38</sup> The fact that this product was not detected for the bulk catalysts may be due to some differences in acid properties between the bulk and supported catalysts, under the reaction conditions. As shown in Figure 4b, furfural selectivity for MP34CsPW is roughly 25% higher than that for MP15CsPW at any given conversion in the range of 50–80%.

Comparing the catalytic results at 4 h for the MP15CsPW and LP15CsPW catalysts (Table 1), no major influence of the pore size on the catalytic activity can be discerned, suggesting that for relatively low PW loadings the pore size is not a primary factor governing the reaction rate (Table 1). On the other hand, furfural yield at 4 h practically doubles when using the large-pore support. The enlarged pores may enable faster diffusion of furfural through the channels and therefore avert its decomposition through consecutive reactions.

A decrease in the reaction temperature of 20 °C (from 160 to 140 °C) causes the reaction rate to decrease by about 50% (based on conversion at 4 h) for the LP/MP<sub>x</sub>CsPW catalysts, and furfural yields decrease to approximately one third of the values seen at the higher temperature (Table 1).

The influence of the solvent was investigated for the supported catalysts by using DMSO or T/W at 140 °C. One advantage of using DMSO is that it is bio-degradable. In DMSO, without HPA, furfural yield is negligible, but xylose conversion reaches 34% after 4 h (Table 1). In the presence of LP/MP<sub>x</sub>CsPW, furfural yields in DMSO are much higher than those in T/W. These results may be due to the solvating ability of DMSO towards cations, that is, the solvent may stabilize the positively charged intermediates of xylose conversion and therefore inhibit their consecutive reactions with furfural into heavy products (e.g., furfural pentose, difurfural xylose<sup>3</sup>). Differences in catalytic activity between the MP15CsPW and MP34CsPW samples (based on conversion at 4 h) are more pronounced in DMSO than in T/W such that the supported catalyst with the higher PW loading exhibits a much higher catalytic activity in DMSO than in T/W (discounting the 'necatalytic' contribution in DMSO). These results may be due to differences in catalyst stability for the two solvent systems.

The stability of the supported catalysts was studied by recycling the solids recovered from reactions in either T/W at 160 °C or DMSO at 140 °C, and by

characterizing the used catalysts. After each catalytic run the solids were separated by centrifugation, and attempts were made to regenerate the catalysts by washing consecutively with MeOH, toluene and acetone, and finally drying at 45 °C. In T/W, loss of catalytic activity is mainly observed between the first and second runs, and this effect seems to be independent of the PW loading or the catalyst support (Fig. 5). This was also observed at the lower temperature of 140 °C. Loss of catalytic activity was accompanied by loss of furfural yield. Washing the solids thoroughly with MeOH and toluene did not have a visible effect since it was generally observed that the initially white solids had turned light brown, suggesting the presence of organic matter on the catalyst surfaces. DSC analyses under air of the used catalysts (after thorough washing and drying) showed a broad exothermic band with an onset at ca. 250 °C that was not exhibited by the fresh catalysts, and may therefore be attributed to the decomposition of included organic matter. Hence, catalyst deactivation is at least partly due to strong adsorption of products. When, for example, the MP15CsPW catalyst was regenerated by heating at 350 °C for 3 h to facilitate desorption of the adsorbed products, the recovered solid regained a white color and loss of activity in T/W decreased from ca. 35% (for the solids recovered without thermal treatment) to ca. 10%. After the third batch in T/W, the PW loading was 78% of its original value ascertained by ICP-AES, indicating that partial catalyst dissolution is another cause of catalyst deactivation for these materials in T/W. However, in DMSO, catalytic stability is much

higher, with practically no loss of activity observed for the LP/MP15CsPW catalysts (Fig. 5).

#### 4. Conclusions

$\text{Cs}_x\text{H}_{3-x}\text{PW}_{12}\text{O}_{40}$  ( $\text{Cs}_x\text{PW}$ ) compounds and cesium salts of 12-tungstophosphoric acid (CsPW) immobilized in medium-pore or large-pore micelle-templated silicas are active catalysts for the cyclodehydration of xylose into furfural, in either a toluene/water solvent system or in DMSO. In T/W, the catalytic results are comparable to those obtained using 0.05 M sulfuric acid (25% furfural yield, at 160 °C). The initial catalytic activities decrease in the order silica-supported  $\text{CsPW} > \text{Cs}_{2.5}\text{PW} > \text{Cs}_{2.0}\text{PW} > \text{HPW}$ . Increasing the CsPW loading from 15 to 34 wt % or using a support with a larger pore diameter nearly doubles furfural yields. A rise in the reaction temperature from 140 to 160 °C practically triples furfural yields. Further optimization of the reaction conditions (the most recent furfural production processes focus on temperatures in excess of 200 °C<sup>3</sup>) and adequate reactor (the heart of the process) design may improve furfural yields. DMSO seems to be a better solvent than the T/W solvent system for xylose-to-furfural conversion using the silica-supported CsPW catalysts, since it leads to higher furfural yields and better catalyst stability.

#### Acknowledgements

This work was partly funded by the FCT, POCI, and FEDER (project POCI/QUI/56112/2004). The authors wish to express their gratitude to Professor C. P. Neto for helpful discussions, Dr. D. Evitiouguine (CICECO) and Dr. F. Domingues (Department of Chemistry) for access to HPLC equipment, and M. F. Lucas for assistance in the HPLC analyses, and Dr. I. Fonseca (FCT-UNL, Lisbon) for providing N<sub>2</sub> adsorption data. We also wish to thank Professor J. Rocha for generous support. A.S.D. and S.L. are grateful to the FCT for grants.

#### References

1. *Biorefineries—Industrial Processes and Products*; Kamm, B., Gruber, P. R., Kamm, M., Eds.; Wiley-VCH: Weinheim, 2006.
2. Lichtenthaler, F. W. *Carbohydr. Res.* **1998**, *313*, 69–89.
3. Zeitsch, K. J. *The Chemistry and Technology of Furfural and its Many By-Products*, 1st ed.; Sugar Series; Elsevier: The Netherlands, 2000; Vol. 13.
4. Lichtenthaler, F. W. *The Key Sugars of Biomass: Availability, Present Non-Food Uses and Potential Future Development Lines*. In *Biorefineries—Industrial Processes and Products*; Kamm, B., Gruber, P. R., Kamm, M., Eds.; Wiley-VCH: Weinheim, 2006; Vol. 2, pp 3–59.

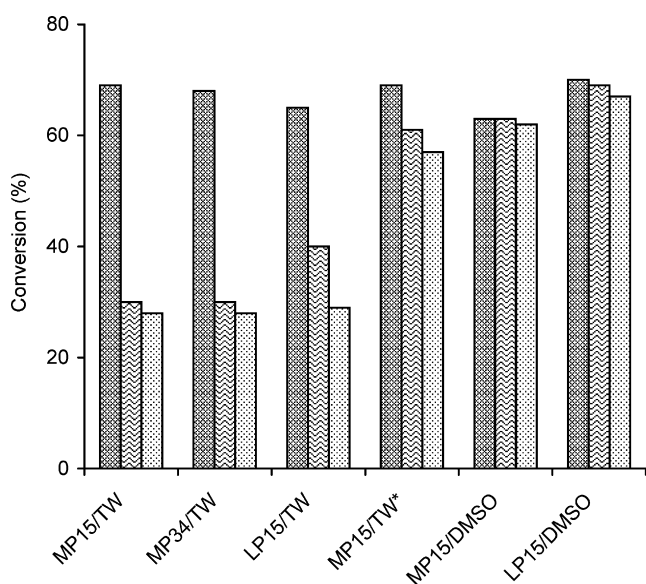


**Figure 5.** Xylose conversion after 4 h reaction in the presence of the MP/LP<sub>x</sub>CsPW (abbreviated MP/LP<sub>x</sub>) supported catalysts, in T/W at 160 °C or DMSO at 140 °C: run 1 (diamonds), run 2 (waves), run 3 (dots). For MP15/TW\*, the recovered solid was calcined prior to reuse in T/W at 160 °C.

5. Horton, B. *Nature* **1999**, *400*, 797–799.
6. Anastas, P. T.; Zimmerman, J. B. *Environ. Sci. Technol.* **2003**, *37*, 94A–101A.
7. Misono, M.; Nojiri, N. *Appl. Catal.* **1990**, *64*, 1–30.
8. Kozhevnikov, I. V. *Chem. Rev.* **1998**, *98*, 171–198.
9. Mizuno, N.; Misono, M. *Chem. Rev.* **1998**, *98*, 199–217.
10. Misono, M.; Ono, I.; Koyano, G.; Aoshima, A. *Pure Appl. Chem.* **2000**, *72*, 1305–1311.
11. Izumi, Y. *Catal. Today* **1997**, *33*, 371–409.
12. Okuhara, T. *Chem. Rev.* **2002**, *102*, 3641–3665.
13. Dias, A. S.; Pillinger, M.; Valente, A. A. *Appl. Catal. A: Gen.* **2005**, *285*, 126–131.
14. Corma, A.; Martínez, A.; Martínez, C. J. *Catal.* **1996**, *164*, 422–432.
15. Okuhara, T.; Watanabe, H.; Nishimura, T.; Inumaru, K.; Misono, M. *Chem. Mater.* **2000**, *12*, 2230–2238.
16. Misono, M. *Chem. Commun.* **2001**, 1141–1152.
17. Haber, J.; Pamin, K.; Matachowski, L.; Napruszewska, B.; Połtowicz, J. J. *Catal.* **2002**, *207*, 296–306.
18. Izumi, Y.; Ono, M.; Ogawa, M.; Urabe, K. *Chem. Lett.* **1993**, 825–828.
19. Essayem, N.; Coudurier, G.; Fournier, M.; Védrine, J. C. *Catal. Lett.* **1995**, *34*, 223–235.
20. Okuhara, T.; Nishimura, T.; Misono, M. *Chem. Lett.* **1995**, 155–156.
21. Okuhara, T.; Nishimura, T.; Misono, M. *Stud. Surf. Sci. Catal.* **1996**, *101*, 581–590.
22. Molnár, Á.; Beregszászi, T.; Fudala, Á.; Lentz, P.; Nagy, J. B.; Kónya, Z.; Kiricsi, I. J. *Catal.* **2001**, *202*, 379–386.
23. Nowinska, K.; Kaleta, W. *Appl. Catal. A: Gen.* **2000**, *203*, 91–100.
24. Choi, S.; Wang, Y.; Nie, Z.; Liu, J.; Peden, C. H. F. *Catal. Today* **2000**, *55*, 117–124.
25. Nunes, C. D.; Valente, A. A.; Pillinger, M.; Fernandes, A. C.; Romão, C. C.; Rocha, J.; Gonçalves, I. S. J. *Mater. Chem.* **2002**, *12*, 1735–1742.
26. Dias, A. S.; Pillinger, M.; Valente, A. A. *Microporous Mesoporous Mater.* **2006**, *94*, 214–225.
27. Lindlar, B.; Kogelbauer, A.; Kooyman, P. J.; Prins, R. *Microporous Mesoporous Mater.* **2001**, *44–45*, 89–94.
28. Wang, Y.; Peden, C. H. F.; Choi, S. *Catal. Lett.* **2001**, *75*, 169–173.
29. Volkova, G. G.; Plyasova, L. M.; Salanov, A. N.; Kustova, G. N.; Yurieva, T. M.; Likholobov, V. A. *Catal. Lett.* **2002**, *80*, 175–179.
30. Dias, J. A.; Caliman, E.; Dias, S. C. L. *Microporous Mesoporous Mater.* **2004**, *76*, 221–232.
31. Soled, S.; Miseo, S.; McVicker, G.; Gates, W. E.; Gutierrez, A.; Paes, J. *Catal. Today* **1997**, *36*, 441–450.
32. Yang, W.; Billy, J.; Taârit, Y. B.; Védrine, J. C.; Essayem, N. *Catal. Today* **2002**, *73*, 153–165.
33. Okuhara, T.; Nishimura, T.; Watanabe, H.; Misono, M. *J. Mol. Catal.* **1992**, *74*, 247–256.
34. Koyano, G.; Ueno, K.; Misono, M. *Appl. Catal. A: Gen.* **1999**, *181*, 267–275.
35. Yoshimune, M.; Yoshinaga, Y.; Okuhara, T. *Microporous Mesoporous Mater.* **2002**, *51*, 165–174.
36. Blasco, T.; Corma, A.; Martínez, A.; Martínez-Escolano, P. J. *Catal.* **1998**, *177*, 306–313.
37. Essayem, N.; Tong, Y. Y.; Jovic, H.; Védrine, J. C. *Appl. Catal. A: Gen.* **2000**, *194–195*, 109–122.
38. Román-Leshkov, Y.; Chheda, J. N.; Dumesic, J. A. *Science* **2006**, *312*, 1933–1937.
39. Antal, M. J., Jr.; Leesomboon, T.; Mok, W. S.; Richards, G. N. *Carbohydr. Res.* **1991**, *217*, 71–85.
40. Okuhara, T. *Catal. Today* **2002**, *73*, 167–176.